

# SUMMER 2021 RESEARCH REPORT

RUOZHEN GONG, EMILY ROSACI, SUSAN WANG

ABSTRACT. As a particle bounces within a macroscopic billiard table, microstructures affect the frequency of output angles. There also exists a connection between macrostructures and microstructures, both of which determining particle behavior, which we quantify as the mean escape time. In the case of a microstructure that introduces specular diffuse collision law, the mean escape time is reminiscent of martingales and optional stopping theorem. With triangular microgeometry, the output angles are finite. We begin to construct the transition matrix which models the behavior of these output angles, and define the ways in which the angles transform within the triangular cells.

## 1. INTRODUCTION

Motivated by its applications in chemical engineering and kinetics, we model the movement of a point particle in a billiard system. That is, within our simulations, a particle moves within a macroscopic table which we define as a channel with parallel walls and a fixed length. The particle interacts with these walls, or boundaries of the billiard table, such that it reflects from the surface at a random angle according to some probability distribution. We can define this system as a *random billiard*, and introduce microstructures to study their effects on particle movement.

In Section 2, we present the existence of a microstructure that introduces specular diffuse collision law to the random billiard system. We examine the movement of a particle within a channel, and determine that the particle's position after a set number of steps takes on a Gaussian distribution. There also exists a relationship between the collision law and the mean escape time which requires further analysis.

We then discuss particle movement within a channel with a geometric microstructure in Section 3. In particular we focus on a collision law that is determined by the particle interacting with a triangular cell whose dimensions are at a scale incommensurate with the scale of the channel. When the triangular cell is isosceles and has vertex angles which are rational multiples of  $\pi$ , the set of possible collision angles is finite. We define four cases in which the particle can enter and exit each cell, and begin to construct the limiting distribution of the transition matrix for the state space of the output angles.

## 2. SPECULAR-DIFFUSE RANDOM COLLISION LAW

We first consider a channel with a microstructure that introduces specular diffuse collision law. In this collision law, the particle can reflect off of the macroscopic walls of the channel in two ways: diffusely or specularly. A *diffuse collision* occurs when the outgoing angle of the particle is selected randomly according to Knudsen's cosine law distribution. The parameter  $\alpha$  determines the probability of this collision occurring. Conversely, a *specular collision* will occur with a probability of  $1 - \alpha$ . In this case, the particle will reflect off of the macroscopic wall at the same output angle as the previous collision [CF20].

In our simulations, the channel has some length  $L$  and a height of 2 units. The particle begins in the center of the channel, which we set as 0, and collides against its walls until traveling length  $L/2$  in the positive or negative direction. Let  $i$  represent the  $i$ th collision.  $X_i$  will then be the horizontal distance that a particle travels between collision  $i - 1$  and  $I$  for each  $i \geq 1$ . We determine  $X_i$  as a function of  $\theta_i$ , or the output angle. That is, the particle will travel some distance according to the function  $X_i = 2\cot(\theta_i)$ . If we then let  $n \geq 1$ , we can return the horizontal position,  $S_n$ , after the  $n$ th collision as such:  $S_n = \sum_{i=1}^n X_i$ . Through simulation, we find that  $E[S_n] = 0$  for various values of  $n$ . Thus, we believe that the expected value of the particle's position after  $n$  steps will be 0 for any  $n$ . We see an example of this in **Figure 1**.

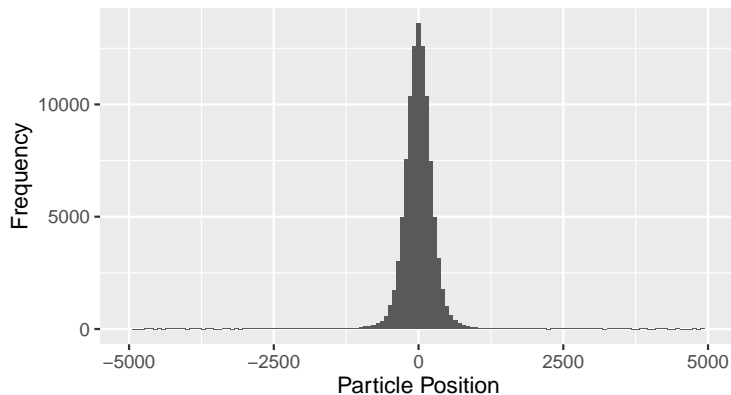


FIGURE 1. After collecting 100,000 particle positions at  $n = 1000$ , we notice the Gaussian distribution with mean 0.

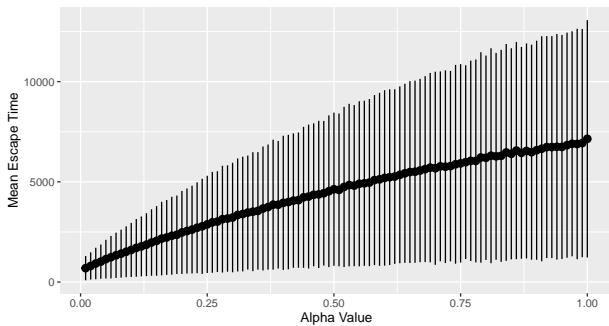


FIGURE 2. Mean escape time from a channel of length  $L = 1000$  units.

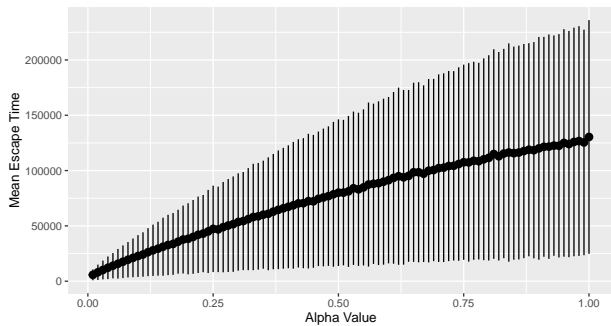


FIGURE 3. Mean escape time from a channel of length  $L = 5000$  units.

We now draw a connection between the macrostructure of the channel and its microstructure by analyzing the mean escape time of a particle. Rather than look at particle positions at step  $n$ , we are interested in the time it takes for a particle to travel to the end of the channel. We define the starting position of the particle to be in the very center of the channel, so the particle can move towards the left exit by travelling a distance of  $-L/2$ , or the right exit

by travelling  $L/2$  in the positive direction. For each trial, we collect the time at the step in which the particle exits, and vary the parameter  $\alpha$  to determine its affect on escape time. Above in **Figures 2** and **3**, we see a definite relationship between  $\alpha$  and mean escape time. Even as we change the length of the channel, we notice a similar shape, though the mean escape time is intuitively greater with a longer channel. The standard error bars in these plots also show an increase in variation of the mean escape time as  $\alpha$  increases.

We expect that the relationship between  $\alpha$  and mean escape time can be explained by the theory of martingales. A *martingale* is a stochastic process in which the expectation remains constant [Dob16]. **Figure 1** displays the type of expectation we would see with a martingale, though we fail to meet the condition of independence between variables as we have defined them so far. This is due to dependence being introduced through the specular collisions, which always repeat the previous output angle. We redefine our stochastic process as follows. Let  $T_i$  for  $i > 1$  be the number of steps between diffuse collisions. The particle will then travel some distance  $X_1 + X_2 + \dots + X_{T_1}$  specularly with  $X_{T_1}$  being the distance traveled by the first diffuse collision. We can further define this total distance as  $Y_1$  such that  $Y_1 = X_1 + X_2 + \dots + X_{T_1}$ . Now, let  $m \geq 1$  where  $m$  can be described as the number of groups of specular collisions until the particle escapes the channel. Then,  $S_m$  is the set of  $Y$  until escaping the channel, and  $S_m = Y_1 + Y_2 + \dots + Y_m$  is a stochastic process with independence among and between its variables.

From here, we hope to further explore  $S_m$  as a martingale, and suspect that the mean escape time has some relationship with optional stopping theorem. However, this is an idea to explore in the future, and we will instead shift our focus to the next microstructure.

### 3. TRIANGULAR MICROSTRUCTURE

We have also discussed the channel with a triangular microstructure. The figure below shows a channel wall with a few triangular cells.

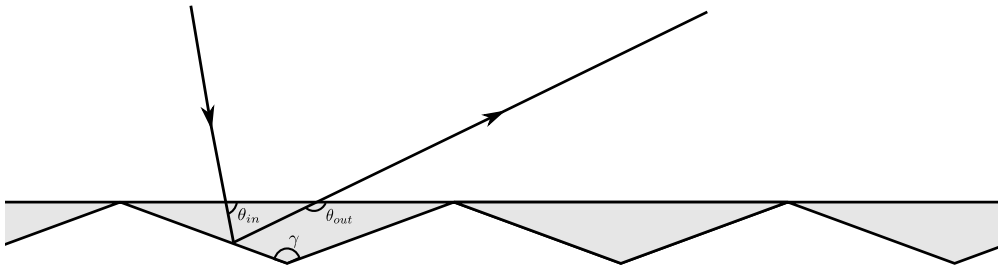


FIGURE 4. Triangular Cells and Angles

As in the figure, we see that the channel consists of small isosceles triangle cells with a 1 unit base side, which we define the vertex angle to be  $\gamma$ . As we follow the particles' trajectories, we define the angle made by the incoming vector (the vector created by the trajectory when entering a cell) and the base of the isosceles triangle to be  $\theta_{in}$ , and the angle made by the outgoing vector (the vector created by the trajectory when entering a cell) and the base of the isosceles triangle to be  $\theta_{out}$ . We find that the value of  $\theta_{out}$  would depend on  $\gamma$  and  $\theta_{in}$ .

When  $\gamma > 2\pi/3$ , there are 4 possible cases for  $\theta_{out}$  with an arbitrary  $\theta_{in}$  and a random position.

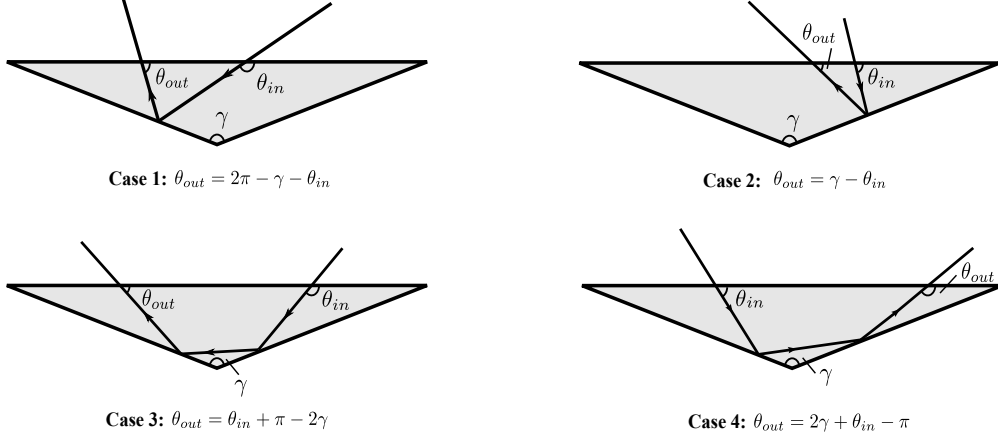


FIGURE 5. Four Possible Cases for  $\theta_{out}$  given some  $\theta_{in}$  and some random position

In the above cases, we find that cases 1 and 2 describe the particle entering the cell and going out by colliding only once, and cases 3 and 4 describe the particle colliding twice to exit the cell. Also, we found through simulation that with the same  $\gamma$  value, different  $\theta_{in}$  determines different case probabilities to  $\theta_{out}$ . For example, when  $\gamma = 3\pi/4$ , and  $\theta_{in} = \pi/2$ , only cases 1 and 2 are possible; but with the same  $\gamma$ , when  $\theta_{in} = 7\pi/11$ , then cases 1, 2, and 3 are all possible.

When a particle enters a channel with the triangular microstructure, it would collide with the channel walls and create a sequence  $\theta_{out}$ 's, as shown in Figure 6

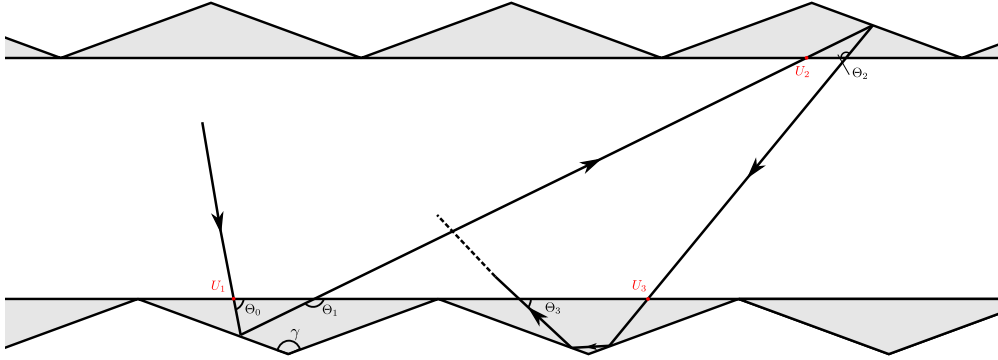


FIGURE 6. A Particle Colliding in a Triangular Microstructure Channel

We let  $\Theta_i$  be this sequence of angles, and define  $U_i$  to be the positions where the particle enters triangular cells each time. As the figure shows, the particle enters the first cell with the initial angle  $\Theta_0$  at position  $U_1$ , and it leaves the cell with angle  $\Theta_1$  and enters another cell later on. Within a channel, the incoming angle of a certain cell is the outgoing angle from the previous cell. For instance,  $\Theta_1$  is the outgoing angle of the first cell but also the incoming angle of the second cell. Thus, we define  $F$  to be the function that will generate the next outgoing angle by collision in the channel,  $F : (0, \pi) \rightarrow (0, \pi)$ . For every choice of  $u$  and  $\theta$ , there's a given angle  $\Theta = F(u, \theta)$ , which is described by one of the four cases shown in Figure 5. Let  $\Theta_n$  be a sequence of random angles for  $n \geq 0$ , and let  $U_n$  be a given i.i.d. sequence of uniformly distributed random variables for  $n \geq 1$ . According to the definition

of  $F$ , we let  $\Theta_{n+1} = F(U_n, \Theta_n)$  for  $n \geq 1$ . This set up gives a description of the particle's flight through a channel. We assumed that the scale of the microscopic triangular cells is incommensurate with the scale of the channel, so a uniformly distributed position  $U$  upon entry to a cell is used to model the uncertainty created by the difference in scales.

Further, we let  $S$  be the set of  $\Theta_i$ 's. By the definition of the Markov Chain,  $\mathcal{S}$  is the state space of the Markov Chain [Dob16]. We've explored questions and come up with several conjectures regarding the size of the state space,  $|S|$ , and how it relates to different parameters.

In general, when  $\gamma = a\pi/b$  and  $\theta_{in} = p\pi/q$  for some rational number  $a/b$  and  $p/q$ , the state space is finite. The size of the state space depends on  $b$ , the denominator of  $\gamma$ , and we observe that the state space when  $b$  is even is different from the state space when  $b$  is odd.

**Conjecture 3.1** (General Case). If  $\theta_{in}$  is some arbitrary rational multiple of  $\pi$ , except for some special choices of  $\theta_{in}$ , then

$$S = \begin{cases} \{(-1)^k \theta_{in} + k\phi : k \in \mathbb{Z} \text{ and } 1 \leq k \leq b\} & \text{if } b \text{ is even,} \\ \{\pm \theta_{in} + k\phi : k \in \mathbb{Z} \text{ and } 1 \leq k \leq b\} & \text{if } b \text{ is odd.} \end{cases}$$

As a result,

$$|S| = \begin{cases} b & \text{if } b \text{ is even,} \\ 2b & \text{if } b \text{ is odd.} \end{cases}$$

To show the difference, we now give an example for each of the two cases. All examples are aided by our simulation, which explores the state space of different Markov chains by generating the set of all possible outgoing angles given the initial condition.

**Example 3.1.** Let  $\gamma = 4\pi/5$  and suppose  $\theta_{in} = \pi/7$ . Then the state space is  $\mathcal{S} = \{2\pi/35, 5\pi/35, 9\pi/35, 12\pi/35, 16\pi/35, 19\pi/35, 23\pi/35, 26\pi/35, 30\pi/35, 33\pi/35\}$ , and  $|\mathcal{S}| = 10 = 2b$ .

**Example 3.2.** Let  $\gamma = 3\pi/4$  and suppose  $\theta_{in} = \pi/7$ . Then the state space is  $\mathcal{S} = \{3\pi/28, 4\pi/28, 17\pi/28, 18\pi/28\}$ . And the size of the state space is  $|\mathcal{S}| = 4 = b$ .

*Proof.* (Incomplete) The four possible cases of  $\theta_{out}$  given some  $\theta_{in}$  can be summarized by the maps defined in [Fer07], where  $T_i : [0, \pi] \rightarrow \mathbb{R}$  is defined by

$$\begin{aligned} T_1(\theta_{in}) &= \theta_{in} + \phi \\ T_2(\theta_{in}) &= -\theta_{in} + 2\pi - 2\phi \\ T_3(\theta_{in}) &= \theta_{in} - \phi \\ T_4(\theta_{in}) &= -\theta_{in} + 2\phi \end{aligned}$$

We want to use induction to show that the claimed state space  $\mathcal{S}$  is closed under operation  $T_i$  when  $b$  is odd. Also notice that  $s\phi \equiv t\phi \pmod{\pi}$  if  $s \equiv t \pmod{b}$  because of the fact  $\phi = (b-a)\pi/b$ .

For the base case, given an initial  $\theta_0 = \theta_{in}$ , the next outgoing  $\theta_1$  could be written as one of the four possibilities using the relationship  $s\phi \equiv t\phi \pmod{\pi}$  if  $s \equiv t \pmod{b}$ :

$$\begin{aligned} T_1(\theta_{in}) &= \theta_{in} + \phi \\ T_2(\theta_{in}) &= -\theta_{in} + 2\pi - 2\phi = -\theta_{in} + (b-2)\phi \\ T_3(\theta_{in}) &= \theta_{in} - \phi = \theta_{in} + (b-1)\phi \\ T_4(\theta_{in}) &= -\theta_{in} + 2\phi \end{aligned}$$

Thus  $\theta_1 = T_i(\theta_0) = \pm\theta_{in} + k\phi$  with the integer  $k \in [1, b]$ ; if  $k \notin [1, b]$ , we can find some  $l \in [1, b]$  such that  $k\phi \equiv l\phi \pmod{b}$ . So  $\theta_1 \in \mathcal{S}$ . For the induction step, we assume  $\theta_n \in \mathcal{S}$ , in other words,  $\theta_n = \pm\theta_{in} + k\phi$  for some integer  $k$ . Then  $\theta_{n+1} = T_i(\theta_n)$ . With the same argument as in the base case, we see that  $T_i(\theta_n) = \pm\theta_n + k\phi$  for some integer  $k \in [1, b]$ , so  $\theta_{n+1} \in \mathcal{S}$ . Thus  $\mathcal{S}$  is closed under operations  $T_i$ ,  $|\mathcal{S}| \leq 2b$ . **(We still need to show the state space contains all of the claimed elements rather than some of them, and prove the even case.)**

□

The general case is not the complete story. There are two special cases. The first special case is simpler and nicer than the general case, because the state space when  $b$  is even can be described in the same way as the one when  $b$  is odd. This special case happens when  $\theta_{in}$  forms a symmetry with the unfolding diagram, as shown in Figure 7 and explained in the geometric proof. When the incoming trajectory generated by  $\theta_{in}$  is parallel to one of the dashed lines in the unfolding diagram, the state space is smaller than the one in the general case, because the incoming trajectory does not form an angle with the dashed line that it is parallel to.

**Conjecture 3.2** (Special case 1). Given  $\gamma = a\pi/b > 2\pi/3$ , where  $a, b \in \mathbb{N}^+$ , if  $\theta_{in}$  equals some multiple of  $\phi = (b-a)\pi/b$ , then the state space  $\mathcal{S}$  of the Markov chain is the finite set  $\{\pi/b, 2\pi/b, \dots, (b-1)\pi/b\}$ .

**Example 3.3.** Let  $\gamma = 4\pi/5$  and suppose  $\theta_{in} = \pi/5$ . The state space is

$$\mathcal{S} = \{\pi/5, 2\pi/5, 3\pi/5, 4\pi/5\}, |\mathcal{S}| = 4 = b - 1.$$

**Example 3.4.** Let  $\gamma = 5\pi/6$  and suppose  $\theta_{in} = \pi/6$ . The state space is

$$\mathcal{S} = \{\pi/6, 2\pi/6, 3\pi/6, 4\pi/6, 5\pi/6\}, |\mathcal{S}| = 5 = b - 1.$$

We'll prove this conjecture using the geometric method.

*Proof.* Starting with a single triangular cell in the channel, let a particle enters and leaves infinitely amount of triangular cells in a channel. By the unfolding method, We can create an infinite unfolding table and a infinitely long incoming vector according to the collisions [Tab05]. Define  $\theta_i$ , where  $i \in \mathbb{N}$  to be the sequence of angles created by the incoming vector and the entry side of each triangular cell, we get infinitely amount of angles. Figure 7 shows the unfolding diagram of a particle colliding in triangular cells with  $\gamma = a\pi/b > 2\pi/3$ .

Let  $\phi = \pi - \gamma$ . According to the unfolding diagram, we see that the entry side of each triangle cell is an rotation of the original one (the cell which the particle first enters) with the angle  $\phi$  or parallel to one of the rotations. The dashed lines in Figure 7 are the entry sides of triangular cells.

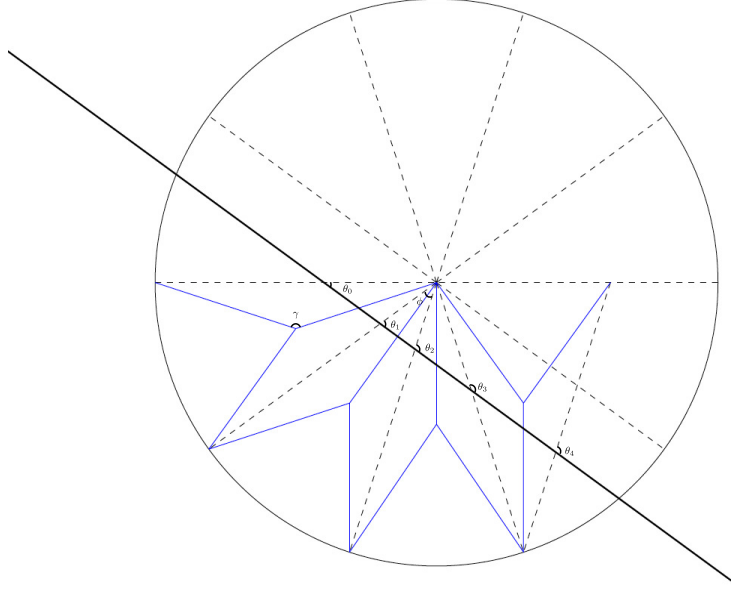


FIGURE 7. The Unfolding Table for Special Case 1

Let all the entry sides be the radii of the circle, we set up a unit circle as shown in Figure 7. Define  $G : (0, 2\pi) \rightarrow (0, 2\pi)$  to be the function that rotates the original entry side  $\pi$ .  $G(\pi) = \pi + \phi$ . Then,

$$\begin{aligned}
 G(\pi) &= \pi + \phi \text{ gives the first rotation,} \\
 G(G(\pi)) &= \pi + 2\phi \text{ gives the second rotation,} \\
 &\dots\dots
 \end{aligned}$$

Let  $k$  be defined as the minimum number of iterations of  $F$  so that

$$G^{(k)}(\pi) = 0.$$

Suppose we've found  $k$ , when  $\theta_{in}$  equals some multiple of  $\phi$ , the incoming vector would be parallel to one of the dashed lines. Thus, the incoming vector can be represented as any of  $\pi + \phi, \pi + 2\phi, \dots, \pi + k\phi$  depending on different values for  $\theta_{in}$ . Thus,  $\theta_i$  equals to the difference of the two formulas representing the dashed line and the incoming vector, which equals to a multiple of  $\phi$ .

For example, Figure 7 represents the unfolding diagram when  $\gamma = 4\pi/5$ , where  $\phi = \pi/5$ . When  $\theta_{in} = \pi/5 = \phi$ , the incoming vector is parallel to the dashed line represented by  $\pi + 4\phi$ . And the dashed lines that have an intersection with the incoming vector are  $\pi, \pi + \phi, \pi + 2\phi, \pi + 3\phi$ . Thus,  $\theta_0 = \theta_{in} = \phi, \theta_1 = 2\phi, \theta_2 = 3\phi, \theta_3 = 4\phi$ . The dashed line that creates  $\theta_4$  is parallel to  $\pi + 2\phi$ , then  $\theta_4 = 2\phi$ .

Since  $\phi = \pi - \gamma$  which equals to a multiple of  $\pi/b$ , then  $\theta_i$  would be a multiple of  $\pi/b$ .

Therefore, given  $\gamma = a\pi/b > 2\pi/3$ , where  $a, b \in \mathbb{N}^+$ , if  $\theta_{in}$  equals some multiple of  $\phi = (b-a)\pi/b$ , then the state space  $\mathcal{S}$  of the Markov chain is the finite set  $\{\pi/b, 2\pi/b, \dots, (b-1)\pi/b\}$ .  $\square$

When the particle trajectory generated by the incoming angle  $\theta_{in}$  is parallel to one side of the triangle as illustrated in 8, only the first two cases of the four possible cases described in Figure 5 is possible. Since the number of possible cases are cut in half, the size of the state space is also half the size of the one in the general case.

**Conjecture 3.3** (Special case 2). Let  $\gamma = a\pi/b > 2\pi/3$ , and  $\phi = \pi - \gamma = (b - a)\pi/b$ . If  $\theta_{in} = \phi/2 + k\phi$  for some integer  $k$ , then

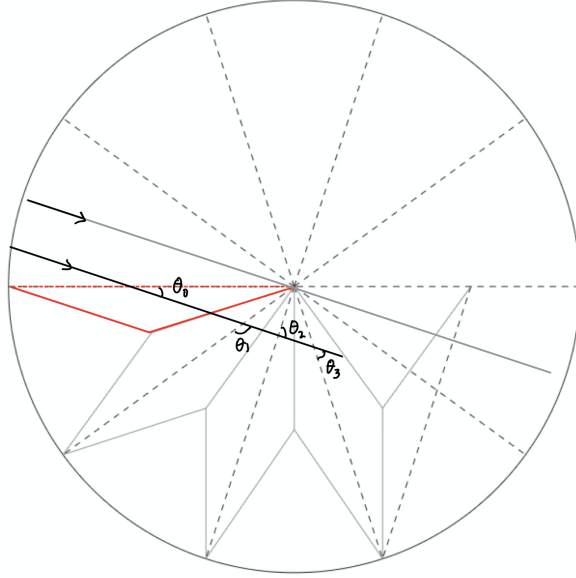


FIGURE 8. The Unfolding Table for Special Case 2

- (1) If  $b$  is odd, the state space is given by  $\mathcal{S} = \{\theta_{in} + k\phi : k \in \mathbb{N}\}$ , and  $|\mathcal{S}| = b$ .
- (2) If  $b$  is even, the state space is given by  $\mathcal{S} = \{\theta_{in} + 2k\phi : k \in \mathbb{N}\}$ , and  $|\mathcal{S}| = b/2$ .

We now give an example for each case.

**Example 3.5.** Let  $\gamma = 2\pi/3$ , then  $\phi = \pi - \gamma = \pi/3$ . Suppose  $\theta_{in} = \phi/2 + k\phi$  for some integer  $k$ . In other words,  $\theta_{in} \in \{\pi/6, 3\pi/6, 5\pi/6\}$ . Then the state space is  $\mathcal{S} = \{\theta_{in} + k\phi : k \in \mathbb{N}\} = \{\pi/6, 3\pi/6, 5\pi/6\}$ , and  $|\mathcal{S}| = 3$ .

**Example 3.6.** Let  $\gamma = 3\pi/4$ , then  $\phi = \pi - \gamma = \pi/4$ . Suppose  $\theta_{in} = \phi/2 + k\phi$  for some integer  $k$ . In other words,  $\theta_{in} \in \{\pi/8, 3\pi/8, 5\pi/8, 7\pi/8\}$ . The state space is  $\mathcal{S} = \{\theta_{in} + 2k\phi : k \in \mathbb{N}\}$ . Namely, when  $\theta_{in} = \pi/8$  or  $5\pi/8$ ,  $\mathcal{S} = \{\pi/8, 5\pi/8\}$ ; when  $\theta_{in} = 3\pi/8$  or  $7\pi/8$ ,  $\mathcal{S} = \{3\pi/8, 7\pi/8\}$ ; and the size of the state space is  $|\mathcal{S}| = 2$ .

The proof of this conjecture should follow from the proof of the general case, since the difference between even and odd  $b$  in this special case is similar to the one in the general case.

Our last conjecture characterizes different cases of the long-term behavior of the Markov chain, which is related to how accessible groups of states are from each other. We introduce the notion of a communication class as defined in [Dob16] before stating the conjecture.



**Definition 3.1** (Communication class). If  $P_{ij}^n > 0$  for some  $n \geq 0$ , we say that state  $j$  is *accessible* from state  $i$ . Then there is positive probability of reaching  $j$  from  $i$  in a finite number of steps. States  $i$  and  $j$  *communicate* if  $i$  is accessible from  $j$  and  $j$  is accessible from  $i$ .

Since communication is an equivalence relation, the state space can be partitioned into equivalence classes, called *communication classes*. Namely, the state space can be divided into disjoint subsets, each of whose states communicate with each other but do not communicate with any states outside their class.

**Conjecture 3.4.** Given  $\gamma = a\pi/b > 2\pi/3$  with  $a, b \in \mathbb{N}^+$ , then

- (1) If  $b$  is even, the Markov chain has a single communication class.
- (2) If  $b$  is odd, the Markov chain has two communication classes.
- (3) If  $\theta_{in} = k\pi/b$  as described in the first special case, the Markov chain has a single communication class regardless of whether  $b$  is even or odd.

We demonstrate examples of the transition matrix  $P$  and  $\lim_{n \rightarrow \infty} P^n$  for the three cases respectively.

**Example 3.7.** Let  $\gamma = 3\pi/4$  and suppose  $\theta_{in} = \pi/5$ . The state space is

$$\mathcal{S} = \{\pi/20, \pi/5, 11\pi/20, 7\pi/10\}.$$

The resulting transition matrix is

$$\mathbf{P} = \begin{matrix} & \pi/20 & \pi/5 & 11\pi/20 & 7\pi/10 \\ \begin{matrix} \pi/20 \\ \pi/5 \\ 11\pi/20 \\ 7\pi/10 \end{matrix} & \begin{pmatrix} 0 & 0 & 0 & 1 \\ 0 & 0 & 0.79 & 0.21 \\ 0 & 0.465 & 0 & 0.535 \\ 0.196 & 0.165 & 0.639 & 0 \end{pmatrix} \end{matrix}$$

$$\mathbf{P}^{160} = \begin{matrix} & \pi/20 & \pi/5 & 11\pi/20 & 7\pi/10 \\ \begin{matrix} \pi/20 \\ \pi/5 \\ 11\pi/20 \\ 7\pi/10 \end{matrix} & \begin{pmatrix} 0.062 & 0.233 & 0.387 & 0.318 \\ 0.062 & 0.233 & 0.387 & 0.318 \\ 0.062 & 0.233 & 0.387 & 0.318 \\ 0.062 & 0.233 & 0.387 & 0.318 \end{pmatrix} \end{matrix}$$

We observe that the limiting distribution of  $P^{160}$  is  $\lambda = (0.062, 0.233, 0.387, 0.318)$ , and it is illustrated in Figure 9.

**Example 3.8.** Let  $\gamma = 2\pi/3$  and suppose  $\theta_{in} = \pi/5$ . The state space is

$$\mathcal{S} = \{2\pi/15, \pi/5, 7\pi/15, 8\pi/15, 4\pi/5, 13\pi/15\}.$$

The resulting transition matrix is

$$\mathbf{P} = \begin{matrix} & 2\pi/15 & \pi/5 & 7\pi/15 & 8\pi/15 & 4\pi/5 & 13\pi/15 \\ \begin{matrix} 2\pi/15 \\ \pi/5 \\ 7\pi/15 \\ 8\pi/15 \\ 4\pi/5 \\ 13\pi/15 \end{matrix} & \begin{pmatrix} 0 & 0 & 0 & 1 & 0 & 0 \\ 0 & 0 & 0.9 & 0.1 & 0 & 0 \\ 0 & 0.534 & 0 & 0 & 0.062 & 0.404 \\ 0.407 & 0.061 & 0 & 0 & 0.532 & 0 \\ 0 & 0 & 0.105 & 0.895 & 0 & 0 \\ 0 & 0 & 1 & 0 & 0 & 0 \end{pmatrix} \end{matrix}$$

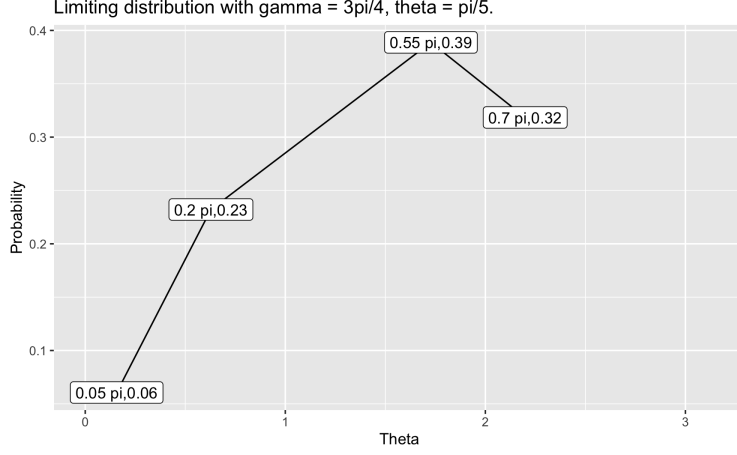


FIGURE 9. Limiting distribution with  $\gamma = 3\pi/4, \theta_{in} = \pi/5$ .

$$\mathbf{P}^{160} = \begin{matrix} & 2\pi/15 & \pi/5 & 7\pi/15 & 8\pi/15 & 4\pi/5 & 13\pi/15 \\ \begin{matrix} 2\pi/15 \\ \pi/5 \\ 7\pi/15 \\ 8\pi/15 \\ 4\pi/5 \\ 13\pi/15 \end{matrix} & \begin{pmatrix} 0.207 & 0.3 & 0 & 0 & 0.289 & 0.204 \\ 0.207 & 0.3 & 0 & 0 & 0.289 & 0.204 \\ 0 & 0 & 0.5 & 0.5 & 0 & 0 \\ 0 & 0 & 0.5 & 0.5 & 0 & 0 \\ 0.207 & 0.3 & 0 & 0 & 0.289 & 0.204 \\ 0.207 & 0.3 & 0 & 0 & 0.289 & 0.204 \end{pmatrix} \end{matrix}$$

to see how the state space decomposes into two disjoint sets of communicating states.

Looking at large powers of  $P$ , we observe that the state space decomposes into two disjoint set of communication states, which is evidence for the claim that the Markov chain has two communication classes when  $b$  is odd.

**Example 3.9.** Let  $\gamma = 4\pi/5$  and suppose  $\theta_{in} = \pi/5$ . The state space is

$$\mathcal{S} = \{\pi/5, 2\pi/5, 3\pi/5, 4\pi/5\}.$$

The resulting transition matrix is

$$\mathbf{P} = \begin{matrix} & \pi/5 & 2\pi/5 & 3\pi/5 & 4\pi/5 \\ \begin{matrix} \pi/5 \\ 2\pi/5 \\ 3\pi/5 \\ 4\pi/5 \end{matrix} & \begin{pmatrix} 0 & 0 & 0.726 & 0.274 \\ 0 & 0.55 & 0 & 0.45 \\ 0.444 & 0 & 0.556 & 0 \\ 0.281 & 0.719 & 0 & 0 \end{pmatrix} \end{matrix}$$

$$\mathbf{P}^{160} = \begin{matrix} & \pi/5 & 2\pi/5 & 3\pi/5 & 4\pi/5 \\ \begin{matrix} \pi/5 \\ 2\pi/5 \\ 3\pi/5 \\ 4\pi/5 \end{matrix} & \begin{pmatrix} 0.193 & 0.302 & 0.316 & 0.189 \\ 0.193 & 0.302 & 0.316 & 0.189 \\ 0.193 & 0.302 & 0.316 & 0.189 \\ 0.193 & 0.302 & 0.316 & 0.189 \end{pmatrix} \end{matrix}$$

The limiting distribution is illustrated by Figure 10.

**Example 3.10.** Let  $\gamma = 5\pi/6$  and suppose  $\theta_{in} = \pi/6$ . The state space is

$$\mathcal{S} = \{\pi/6, 2\pi/6, 3\pi/6, 4\pi/6, 5\pi/6\}.$$

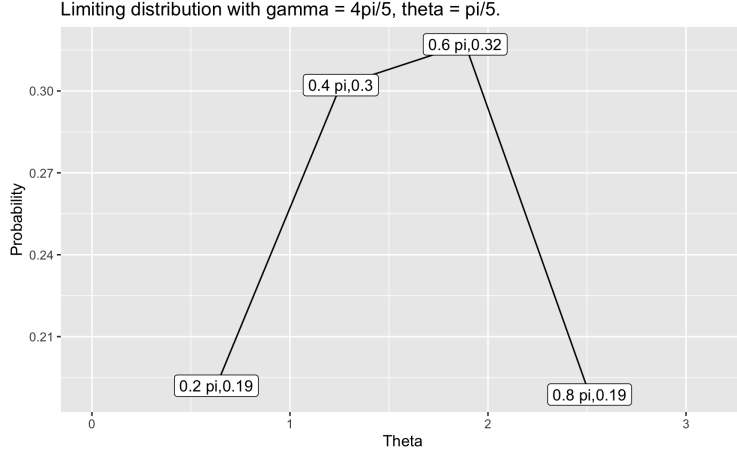


FIGURE 10. Limiting distribution with  $\gamma = 4\pi/5, \theta_{in} = \pi/5$ .

The resulting transition matrix is

$$\mathbf{P} = \begin{matrix} & \pi/6 & 2\pi/6 & 3\pi/6 & 4\pi/6 & 5\pi/6 \\ \begin{matrix} \pi/6 \\ 2\pi/6 \\ 3\pi/6 \\ 4\pi/6 \\ 5\pi/6 \end{matrix} & \begin{pmatrix} 0 & 0 & 0 & 0.735 & 0.265 \\ 0 & 0 & 0.586 & 0 & 0.414 \\ 0 & 0.5 & 0 & 0.5 & 0 \\ 0.426 & 0 & 0.574 & 0 & 0 \\ 0.272 & 0.728 & 0 & 0 & 0 \end{pmatrix} \end{matrix}$$

$$\mathbf{P}^{160} = \begin{matrix} & \pi/6 & 2\pi/6 & 3\pi/6 & 4\pi/6 & 5\pi/6 \\ \begin{matrix} \pi/6 \\ 2\pi/6 \\ 3\pi/6 \\ 4\pi/6 \\ 5\pi/6 \end{matrix} & \begin{pmatrix} 0.136 & 0.23 & 0.269 & 0.234 & 0.131 \\ 0.136 & 0.23 & 0.269 & 0.234 & 0.131 \\ 0.136 & 0.23 & 0.269 & 0.234 & 0.131 \\ 0.136 & 0.23 & 0.269 & 0.234 & 0.131 \\ 0.136 & 0.23 & 0.269 & 0.234 & 0.131 \end{pmatrix} \end{matrix}$$

The limiting distribution is illustrated by Figure 11.

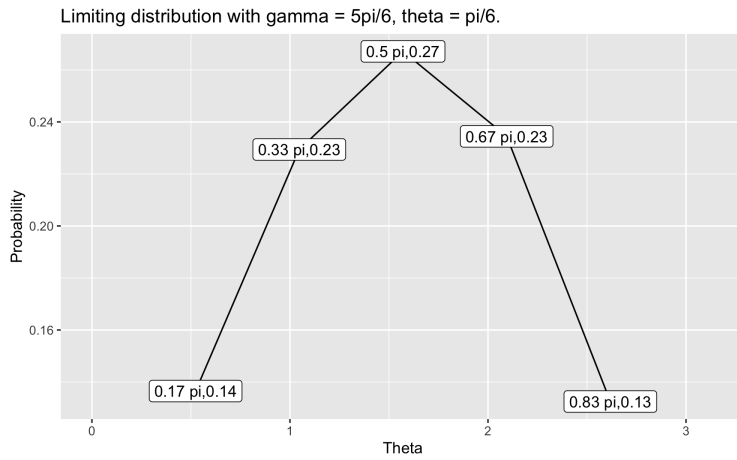


FIGURE 11. Limiting distribution with  $\gamma = 5\pi/6, \theta_{in} = \pi/6$ .

#### 4. FURTHER QUESTIONS

This summer, we have studied the specular-diffuse random collision model and the triangular microstructure as two rather parallel threads. Looking forward, we hope to further our understanding for both models and build connections between them.

For the specular-diffuse random collision model, we plan to investigate how mean escape time of the particle depends on the parameter  $\alpha$  using martingales and optional stopping theorem.

For the geometric microstructure random collision model, after we have finished proving the finite state space of the Markov chain of possible angles of the particle in the triangular microstructure, we plan to investigate the relationship between the second largest eigenvalue on  $\gamma$  and the mean escape time of particles in the triangular microstructure. We are also interested in other geometric microstructures, like higher order polygons. We expect that similar patterns should emerge in the unfolding diagram of other polygons. We may also look at different microstructures like the circular bumps microstructure, where the Markov chain has an infinite state space.

Eventually, we hope to be able to represent particle behaviors in the geometric microstructures with the specular-diffuse random collision model. In other words, we hope to find a map from parameters like  $\gamma$  in the geometric microstructure to the parameter  $\alpha$  in the specular-diffuse collision model.

## REFERENCES

- [CF20] Timothy Chumley and Renato Feres. “Exact Discretization of Harmonic Tensors”. In: *Discrete Contin. Dyn. Syst.* (2020).
- [Dob16] Robert P. Dobrow. *Introduction to Stochastic Processes with R*. Hoboken, New Jersey: John Wiley and Sons, 2016.
- [Fer07] Renato Feres. “Random Walks Derived from Billiards”. In: *MSRI Publications* (2007).
- [Tab05] Serge Tabachnikov. *Geometry and billiards*. Vol. 30. American Mathematical Soc., 2005.